Linking Electrochemistry, Modern Aluminium Cell Design and Operating Conditions, for a Better Understanding of Anode Reactions and Various Levels of PFC Co-evolution

Part 2: The Impact of Cell Design and Process Conditions on Energy Utilization and PFC emissions and general cell Performance.

Barry Welch[1] and David Wong[2]
1. Professor, University of N.S.W, Sydney, Australia & Consultant,
Welbank Consulting Ltd, New Zealand
2. Manager Project Delivery & Principal Engineer Environmental, Light Metals Research Centre,
University of Auckland, Auckland, New Zealand.
Corresponding author: barry@barry.co.nz

Abstract

This paper is Part 2 of 2 and builds on the improved understanding of the electrochemical and anode reactions (Part 1) and deals with the impact of these changes in aluminium cell design and process conditions over time. With the generally higher operating current densities in modern aluminium reduction cells the anode potential at a fixed alumina concentration is higher. Consequently, because control systems rely on modulating the average dissolved alumina concentration in the cell, there is a much higher risk of the interfacial electrode potential increasing to a value above the limit that is necessary to enable co-evolution of PFCs. The problem is magnified by the increased time-lag required for dissolution and distribution of alumina when fed at a higher rate. Furthermore, extracting the increased amount of heat required during the over-feeding cycle from the surrounding electrolyte becomes more difficult because of the reduced electrolyte volume in modern cell designs. This means that the mixing requires high transverse electrolyte velocities under the anodes and these cannot be readily achieved in modern cells with slotted anodes. Examples that will be presented include undetected low level PFC co-evolution, uneven consumption rate of anodes – sometimes even leading to anode spike formation – and a generally higher process energy consumption.

Keywords: Aluminium reduction, PFC co-evolution, cell design, process conditions, energy consumption.

1. Introduction

As discussed in Part 1, the quality of raw materials and operating conditions determine the range of products that are evolved from anodes in cells. We have also seen that limitations, work practices and control practices cause further deviations from target operating conditions and can aggravate the situation. Throughout the history of aluminium smelting there have progressively been changes in cell design and operating practices in order to overcome weaknesses and achieve the goals of the smelter.

Cell performance is measured against many different parameters such as current efficiency (CE%), energy consumption, cell life, operating cost, capital cost, metal quality, and environmental performance. Frequently the emphasis of developments has been biased towards whichever of these parameters has the greatest needs. By integrating design advances with better fundamental understanding, improved process control and better materials available, there has been spectacular progress as seen in Table 1. The data included in Table 1, is compiled from

operating records made available to the authors for a large range of cell design and technologies encompassing the full period of commercial aluminium production.

In the last two decades environmental performance has become much more important. With that there has also been a linked driver to reducing energy consumption per unit production because of the scarcity of electrical energy that has a low greenhouse gas footprint. Published papers and press announcements associated with performance of new technologies being developed in test groups by Hydro and Rio Tinto indicate that there is an ability to design and operate cells at and even below the 12 DC kWh/kg Al barrier. However, these are not included in Table 1 due to the absence of long-term, complete potline operating data as the respective technologies are only in operation for a limited amount of time.

Table 1. Typical key performance indicators (KPIs) of Selected leading cell technologies for the era.

KPI Era ± 10 yrs	**Units**	***The Changing Performance Indices***				
		1920	1955	*1955* Søderberg*	1985	2015
Cell Size	kA/cell	14	55	*100**	180	> 420
Gross Carbon Consumption	kg C/kg Al	0.65	0.58	*0.54*	0.5	0.5
Net Carbon Consumption	kg C/kg Al	0.58	0.47	*0.54*	**0.405**	0.42
Current Efficiency (CE%)	% theoretical	77	83	*85*	**95.5**	94
Energy Consumption	DC kWh/kg Al	22	16	*16*	**12.7**	13
Anode Effect Frequency	AE/cell-day	3.5	3	*3*	0.35	**0.03**
Cell Life	Days	500	700	*700*	**3000**	2000
Environmental Issues	Type		Fluoride SO_2 and dust	Fluoride, SO_2 dust and PAHs		**PFCs co-evolving**

1.1. Brief Historical Trend of Technology

The above table shows that the most recent technology has shifted in a manner that some of the key performance indicators (KPIs) are below those achievable earlier. Therefore, in order to understand the technological changes so that the best path can be developed for future metal production, this paper reviews some of the key technical changes that have happened, followed by an assessment of their impact.

The Søderberg technology introduced in the early 1920s a major capital expenditure advantage by eliminating the need for an anode plant and its associated facilities. It also proved to be very beneficial on work practices by eliminating the need for anode change whilst it also enabled a significant increase in operating line current. Consequently it expanded rapidly especially during World War II when there was a high demand for aluminium. No new potlines using Søderberg technology has been installed in the Western world for more than 30 years because their energy efficiency, environmental footprint and carbon consumption will always lag that of prebaked cell technology through technical reasons.

The major step in the improvements occurred in the period between 1955 and 1985. During this period there had been intensive R&D at many smelters in order to address the harmful fluoride emissions and eliminate problems that lead to performance deterioration. But equally important, it coincided with the explosion in solid-state electronics and the digital era. For example,

following the publication of the relationship between Al_2O_3 concentration and cell voltage for different operating conditions [1], alumina feed control strategy was introduced for both better cell stability and also to eliminate the formation of sludge. Point feeders delivering small masses of alumina at any one time were introduced aiding alumina dissolution and limited predictive control over alumina concentrations. During this period there was also an "oil crisis" with predictions of there being severe limitations of future supply, and therefore there was an industrial emphasis on energy efficiency. Hence the technologies involved and included in the 1985 column had the best set of KPIs that have been achieved by the industry.

There are three other interesting features associated with Table 1:

I. Other than productivity per cell, the latest technologies in 2015 have inferior KPIs for some of the measures compared with what was achievable 30 years earlier.
II. An extremely undesirable environmental issue, PFC co-evolution during normal operating conditions, has become a common feature in all large modern cells. *Whether this existed earlier is questionable since its detection has been enabled by modern instrumentation and cell monitoring.* PFC emissions from anode effects (AEs), however, have been reduced significantly since the 1950s, a testimony to the industry's major efforts to reduce the frequency and duration of these events.
III. While not shown in the table, all the technologies operating today are running at line currents at least 20 % higher than what the pot shell and cathode technology were originally designed for.

Figure 1. Illustration of the change in anode sizes (from 1 to 7) used in cells originally designed for 55 kA to enable line current increase.

Typical brownfield retrofits that have been applied to cell technologies over the years are:

- Increase in the physical size of anodes with respect to both their 'shadow' over the cathode and total mass – to enable higher amperage without severe impact on anode current density, and simultaneously reduce the frequency with which the anodes need to be changed.
- Self-sealing modifications to the cathode current collector bar design and materials selection for the same reason – lowering ohmic resistance.
- Reduced thickness of the cathode sidewall materials with the use of higher thermal conductivity materials (silicon carbide refractories) to accommodate larger anodes and simultaneously encourage formation of the self-sealing protective side ledge.
- Reduction in the gap between anodes in the centre channel, again to accommodate the larger anodes.

- Changed anode setting patterns to enable better and more reliable anode covering in order to eliminate extraneous anode consumption reactions (such as air burning) and often simultaneously increasing the mass or number of anodes being changed at any one time.
- The slotting of anodes to reduce the electrolyte resistance by aiding the release of the anode gas and thus having a smaller average residence volume of the gas that is electrochemically generated.
- Changing alumina feeding strategies, from the original side-breaking off massive amounts – in excess of that possible to dissolve in the electrolyte – to point feeders that add small amounts of alumina at any one time to the centre channel electrolyte, which has enough thermal energy capacity to provide the heat necessary to achieve operating temperature and dissolve.
- Automating the alumina feed strategy following development of the fundamental relationship between cell voltage change, interelectrode distance, and dissolved alumina concentration.
- Increasing the size of the cells to more efficiently use the automation equipment and lower unit capital cost and this is consequentially associated with an increase in line amperage. Larger cells also reduce the cell heat loss, which represents wasted energy.

As the benefits of each of these retrofits have been proven, new larger cell designs have evolved. These usually incorporate a re-design of the electrical circuitry layout to minimise the distortion of the metal pad caused by the higher DC current flow – but not for the subsequent current creep.

All new greenfield smelters installed over the last decade have at least 36 anodes in their cells, ranging to 56, and operate at line currents between 410 kA and in excess of 600 kA. The increase in amperage has generally been associated with an increase in length of the cells rather than any significant widening. One side effect of this evolution is that modern cells are more prone to transgressing to have zones where spatially they enable periods where co-evolving perfluorocarbons can occur under apparently normal operating conditions and they have a new range of problems that were rarely encountered 40 years ago.

Another common feature of the operating technologies is that they are operating with line amperages that invariably have been increased between 10 and 20% higher than the original design, usually by increasing the anode size.

2. The Impact of Retrofits on Cell Conditions, Operation and Performance

The energy applied ***to the cell*** is given by the following relationship:

$$I \times V_{\text{“at cell”}} = I \times \left(E_{anode} + E_{cathode} \right) + I^2 \times \left(R_{anode} + R_{cathode} + R_{bath} \right) \quad (1)$$

where I is the line amperage, $V_{\text{“at cell”}}$ is the voltage across a cell excluding external bus-bar voltage drops, E_{anode} and $E_{cathode}$ are the anode and cathode potentials, respectively, while R_{anode}, $R_{cathode}$ and R_{bath} are the ohmic resistances of the anode, cathode and electrolyte, respectively.

And this energy contributes to three aspects of smelter cell operations:

- Normal cell heat loss – which is strongly design dependent.
- Energy to preheat the materials added to the required state (e.g. dissolved alumina) in the cell.
- Energy for all the chemical reactions that occur within the cell.

These values set the resulting cell voltage necessary after allowing for the current efficiency, and the impact of the cell-to-cell busbar resistance (I x R_{busbar}).

We have the well-established performance relationship for DC energy consumption:

$$\text{DC kWh/kg Al} = \frac{298 \times V}{CE(\%)} \tag{2}$$

where V is the cell-to-cell voltage, as given by the relationship $V = V_{\text{"at cell"}} + I \; x \; R_{busbar}$; and *[CE%]* is the current efficiency.

Hence, we need to assess how various design changes impact the resulting productivity and performance, which are controlled by these relationships, but at the same time be responsible with respect to environmental issues.

A feature ignored by most operators is the combination of the heat balance constraint and equation (2), resulting in it being impossible to achieve minimum energy consumption at maximum current efficiency. While current efficiency tends to be independent of anode-cathode distance (ACD) at large spacing, it starts an exponential rate of decay below a value that depends on the design and operating practices.

2.1. Increasing the Mass of Carbon Anodes in the Cell

The primary purpose for increasing the mass of carbon anodes in cells has been to enable increased productivity through higher line current while minimising any increase in operating anodic current density. Generally the length and width of the anodes have been maximised, subject to the work practice constraints of anode change. This has had the following two consequences:

- By displacing the electrolyte in the centre and cell side channels, the available volume is decreased and because of that and associated ACD reduction the electrolyte mass is reduced.
- The transient heat demand for preheating newly set anodes to operating temperature has increased substantially.
- Martin and co-workers [2] have monitored the impact of the changes in cell conditions as they have increased their cell size and productivity for technologies when using the various changes highlighted above. As seen in the graph from their publication (Figure 2), the electrolyte volume per kiloamp has been reduced three fold with their technology design gross while each point feeder has had almost trebling of the workload for delivering alumina.

Typically smelters are operating with only 30% of the electrolyte volume they had at the time of introduction of low anodic current density, low energy point-fed cells in the early 1980s. While the anode size has displaced some of the electrolyte, another major contributor has been the necessary reduction in anode-cathode distance (ACD). Typically modern cells have ACDs less than 60% of the common value when benchmark performances were achieved for smelters. While some voltage savings have been achieved through less resistive cathodes and current collector bars, the ACD reduction is also necessary to reduce the heat generation to enable retention of side-ledge.

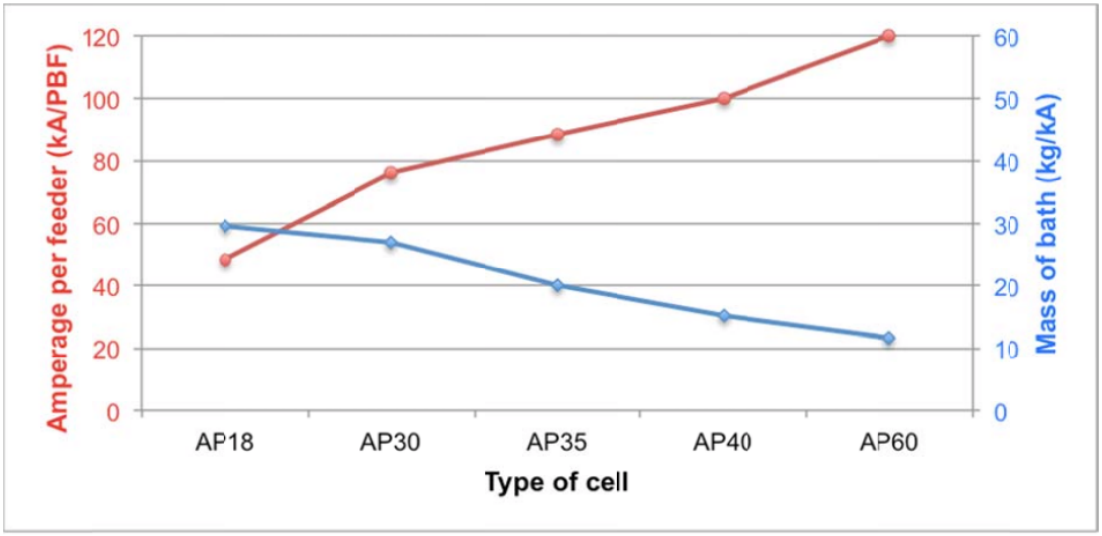

Figure 2. Change in the workload of point feeders and relative reduction in electrolyte mass as a consequence of design and retrofit changes for the technology, according to Martin et al. [2].

2.2. Anode Mass and Current Pickup

As newly set anodes extract heat from the electrolyte, it forms a cryolite-rich freeze in the gap between the undersurface and the metal pad, and also freezes electrolyte around its periphery and within slots. Thereafter they have a slow, conductive heat flow from the metal pad through the frozen bottom layer in the ACD, and from the electrolyte. Simultaneously convective flow of electrolyte aided by anodically evolved gas from the adjacent anode also dissolves the freeze around the sides of the newly immersed anode. In earlier technology the freeze on the side of the anodes would disappear fast, and typically the anode would have 50 % of its target current within the first 6 hours and achieve full current after approximately 12 to 16 hours. With the advent of slots (particularly those in the longitudinal direction of the anode), the reduced agitation of the electrolyte has slowed down dissolution of the side-freeze and associated current pickup on the vertical side. The freeze on the undersurface, having a higher melting point than the electrolyte, also requires convective flow of electrolyte to dissolve. As a consequence of the reduced ACD and smaller anode gas bubles this results in a slower oveall dissolution rate. Consequently this has resulted in the three-part current pickup curve, and seldom do anodes achieve more than 80 % of their target current after 24 hours, usually taking at least 48 hours for full current. Figure 3 presents examples of the two types of curves, and also compares a modern slow current pickup with a cold anode vs. that achieved when the anode had been preheated to 300 °C. From 24 hours to 48 hours, the curves can be extrapolated linearly, but occasionally the rate of increase coul vary with problems and superheat in the cell.

There are three important consequences of the slower current pickup:

a. It increases spatial variation in cell conditions through blockage of the electrolyte flow.
b. It now experiences longer period of high anodic current density and hence individual anode potential of anodes sharing the current load.
c. A greater time that the metal pad profile is distorted through the changed magnetic field.

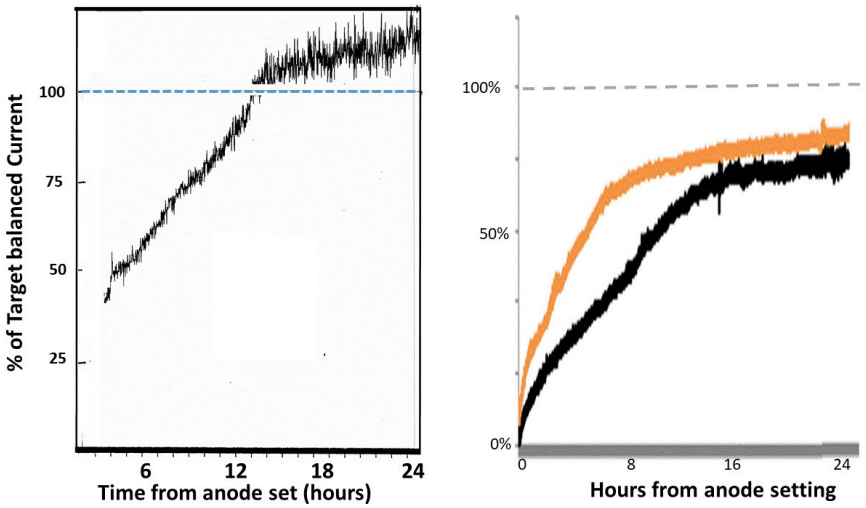

Figure 3. The change in anode preheat rate with slotting and increased mass on [Left] an older cell technology and [Right] a modern cell with cold (black) vs. preheated anodes (orange).

With respect to the third consequence, the magnitude and consequential impact will depend on the anode setting pattern and practice. This is illustrated in Figure 4 for a large cell operating under high productivity conditions (amperage increase 20 % above design) with enlarged anodes. It has a measured metal pad heave that is conforming to its model of only ± 3 cm under stable operations as given by the blue line under one of the rows of anodes.

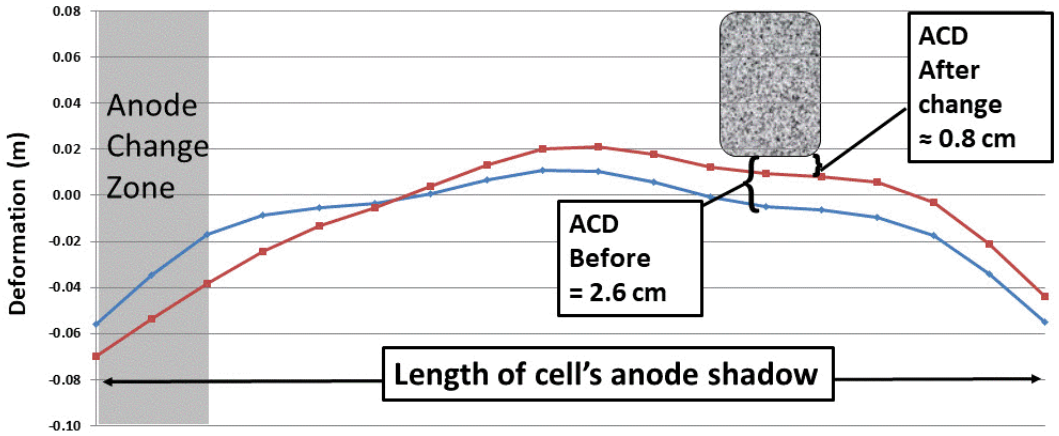

Figure 4. The impact of a selected anode-set on metal pad distortion and resulting anode-cathode spacing.

The red curve represents the model-based calculation of the impact of the anode change that results from the redistribution of current and changed magnetic field as a result of that. For a short period the anode-cathode distance would be about one-third of what it was prior to the change. This results in:

- A higher anodic current density through the reduced ACD, and hence a higher anode potential.
- A reduced rate of delivery of alumina to the affected anode of the reduced electrolyte cross-sectional area.

Consequently the anodes impacted by the anode set have a higher probability of its potential exceeding that is necessary to initiate PFC co-evolution without an AE occurring.

2.3. Dissolving the Freeze under the Anode Surface

While the freeze formed on the sides of the anodes tended to dissolve fast because of the electrolyte agitation of gases evolved on adjacent anodes, the freeze formed on the undersurface is cryolite enriched because of the freezing process and needs to be dissolved by the circulating electrolyte. Studies have shown that it tends to dissolve faster from the centre channel towards the back channel but is retarded because of the absence of electrolyte flowing under the anode and limited liquid electrolyte flow in the side-channel. The last part to disappear is usually towards the back of the anode and this has led to an increase in spike formation and short-circuiting at the rear of the anodes.

Because of the anode consumption through early current pick-up towards the centre channel, the other thing that happens is that the anodic current density will be higher, thereby rapidly depleting the limited alumina concentration and increasing the anode potential further to the point where PFC co-evolution is enabled on the back part of the anode. Again, without an AE occurring.

Lastly, as seen in section 3, for aged cathodes any localised increase in heat generation will result in loss of the limited ledge, thereby enabling sodium deposition and intercalation into the bare carbon and making the electrolyte rich in aluminium fluoride. A situation that is also likely to enhance low level PFC co-evolution!

2.4. Anode Mass, Design and Electrolyte Flow/Mixing

The diagram represented in Figure 2 from Martin et al. [2] also highlights that generally the load on each point feeder has increased substantially. Early research by Purdie et al. [3, 4] on cells operating with ACDs in excess of 4.5 cm showed that for optimum alumina dissolution and mixing adequately within the electrolyte to maintain uniformity of conditions, required at least one point feeder per 50 kA. The practical operation through capacity creep now tends towards one point feeder per 75 to 100 kA. For good operations the higher limit requires electrolyte flows at twice the rate of the optimum. However, with only one-third of the electrolyte volume left the required flow rate goes up more than two-fold.

There are two driving forces for electrolyte mixing:

- Gas pumping by release of large bubbles from the undersurface.
- Electrolyte drag induced by the magnetic forces on the circulating metal pad.

Earlier studies showed that the gas pumping force was the dominant force. More recently, however, anode slots have become an industry standard in order to prevent the growth of large bubbles on the undersurface of the anode and hence the slots reduce the resistance of the electrolyte cross-sectional area in the ACD. When the slots are deeper than the immersion depth of the anode, then the driving force from bubble flow becomes virtually zero.

When we compare metal pad and electrolyte velocity profiles from the output of models, typically the electrolyte velocities are about 10 % of the metal velocities. However, they surprisingly follow a similar pattern as metal velocities. Figure 5 shows a model electrolyte flow output for a modern smelting cell.

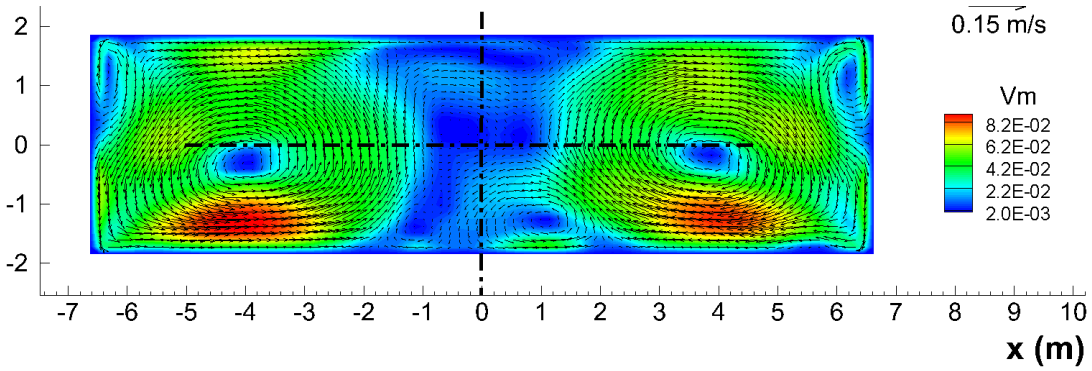

Figure 5. The model output profile of electrolyte flow pattern and velocities in a modern high amperage smelting cell.

The first obvious surprise is that there is not much longitudinal flow of electrolyte in the centre channel where the alumina is added. Added to that is the observation that there are stagnant zones. The efficiency of mixing is going to be extremely dependent on the precision of the positioning of the point feeders, but even so it is indicative that it will be difficult to get homogeneous mixing. Furthermore, this pattern would only be applicable to the electrolyte under the anodes, which is approximately 50 % of the electrolyte in the cell. The anodes act as baffles for the remainder and because recently set anodes have frozen bath material extending underneath the anode surface to the metal pad, electrolyte flow is almost totally inhibited. Therefore, as illustrated in Figure 6, it is not surprising that there are zones in an operational cycle where there is insufficient electrolyte supply. This is supported by the fact that the highest frequency of anode effects in cells occur soon after the anode set is completed. The data taken from cells in one plant is given in Figure 6.

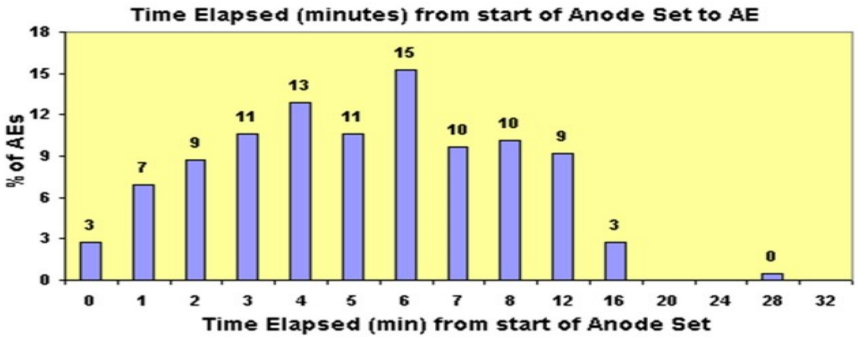

Figure 6. The increase in rate of anode effects associated with anode change through poor electrolyte mixing.

2.5. Mixing and Alumina Dissolution

Aluminium smelter operators excel at playing the "blame game" with any problem undoubtedly arising from the quality of their raw materials and in line with this recently there has been another resurgent of measuring alumina dissolution kinetics. Previous studies showed that, like dissolving sugar or salt in an aqueous solution, mass transfer conditions dominate the kinetics. Granular material added at the same temperature will dissolve faster:

- The more the particles are dispersed,
- The more the mixture is agitated so that the interfacial concentration gradients are minimised, and
- The more the alumina concentration in the electrolyte is displaced from its saturation value.

And for alumina:

- It is essential to have cryolitic anions (AlF_6^{3-}) present to dissolve it.

Based on this alumina dissolution can simply be represented by the following generic rate equation:

$$Dissolution\ Rate\ =\ k_m A_{contact} \left[Na_3 AlF_6 (l) \right]^n \left[C_{Al_2O_3,\ Sat} - C_{Al_2O_3,\ Electrolyte} \right] \quad (3)$$

which encompasses all the variables. The dissolution rate constant k_m can be impacted by the physics of the process, especially its ability to extract heat from the electrolyte. [$C_{Al2O3,\ Sat} - C_{Al2O3,\ Electrolyte}$] is the difference between saturation and actual electrolyte concentrations of alumina, [$Na_3AlF_6\ (l)$] is the mass of liquid electrolyte, n is the order of electrolyte dependence. $A_{contact}$ is the contact surface area.

The unique aspect for alumina dissolution is that it is added cold while it has a high heat of dissolution. This means that the energy to preheat and dissolve alumina must be transferred from the electrolyte it comes in contact with. Table 2 presents the breakdown of options for energy supply allowing for a 10 °C drop in the electrolyte temperature to supply the energy.

Table 2. Options for providing the energy to preheat and dissolve 1 kg of alumina.

Heat supply/sink	**Amount (kg)**	**Initial Temp. (°C)**	**Final Temp. (°C)**	**Energy Required/ released (MJ)**
Heat Demand				
Al_2O_3(gamma) preheat	1	25	960	0.87
Al_2O_3(s) to dissolve	1	960	960	1.06
Total required				1.93
Heat Supply				
Na_3AlF_6(liquid)* by cooling	102	970	960	-1.93
Na_3AlF_6(liquid) by cooling and freezing	3.3	970	960	-1.93
**Typical electrolyte is represented as cryolite for simplicity*				

Monitoring of the temperature in a point feeder hole [5] (underfeed cycle of a low productivity cell) in Figure 7 shows that the electrolyte provides a limited amount of heat quickly, but much of the early heat energy is provided by cryolite freezing onto the alumina. Thereafter, conduction of heat from the metal pad and bath mixing helps the recovery, but the alumina dissolution is retarded and sometimes inhibited by the need to acquire heat for melting the frozen cryolite.

With the modern retrofits the typical dimension changes lead to a volume reduction by about two-thirds of the original amount of electrolyte available to supply the heat and dissolve the alumina. In addition, the agitation and flow of the electrolyte when anodes are slotted, will be reduced and this will further risk slowing the alumina dissolution down. Therefore, spatial variation in cell conditions in different zones will inevitably be enhanced. Since localised low alumina concentrations result in higher individual anode potentials, the cells will transgress into the conditions that enable co-evolution of PFCs more frequently.

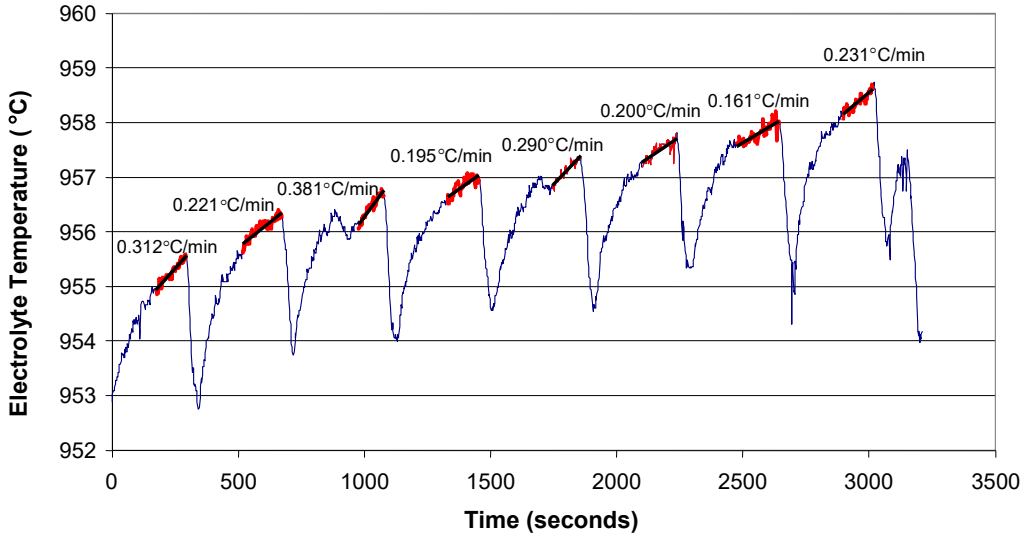

Figure 7. The limitations in temperature drop in the electrolyte in the proximity of the point feeder during an underfeed cycle [5].

2.6. Transverse Alumina Concentration

We have already seen from modelling studies that transverse flow velocities of the electrolyte are low. Furthermore, doubts raised by the reduction in the driving forces through the introduction of anode slots would indicate that the model is likely to overpredict velocities. Today, each point feeder typically sustains an average of 75 kA supplying an equivalent to 100 000 cm² of anode surface. This requires the addition of an average of ~1 kg Al_2O_3 every minute and with it mixing over a transverse radius of approximately 1.8 m after dumping the alumina from the point feeder, which means there is a minimum of 20 seconds for it to disperse within the centre channel and simultaneously dissolve before it is available for mixing in the transverse direction.

In the earlier days, when the cells had 50 kg of electrolyte per kA, then for a 2.5 wt.% Al_2O_3 concentration electrolyte the change in concentration between the successive feeds of alumina was less than 0.027 %. Today, with only one third of that mass of electrolyte, the rate of change is three times faster and the concentration change is greater than 0.08 % Al_2O_3 per minute. *The serious question this introduces is: – is the mixing of the fresh feed alumina getting uniform across the full length of the anode within 40 seconds or not?*

The impact of the electrolyte volume changes is illustrated in Figure 8, which presents the voltage change of a cell with the old technology as its alumina concentration is depleted when not feeding.

As the above cell went to an anode effect at ~780 seconds and the typical design voltage rise for triggering the initiation of an overfeed was 50 mV, it becomes much easier for an individual anode to enter the zone of PFC co-evolution following any alumina feeding irregularities. Perhaps more important, with only a small concentration change needed together with poor mixing of the electrolyte, it becomes easier for alumina concentration gradients to be established under an individual anode. When that occurs the localised anode potential can readily exceed that necessary for co-evolution towards the periphery of the anode. For this there is evidence to support this occurring in some cells – as supported by the sodium co-deposition described in the next section.

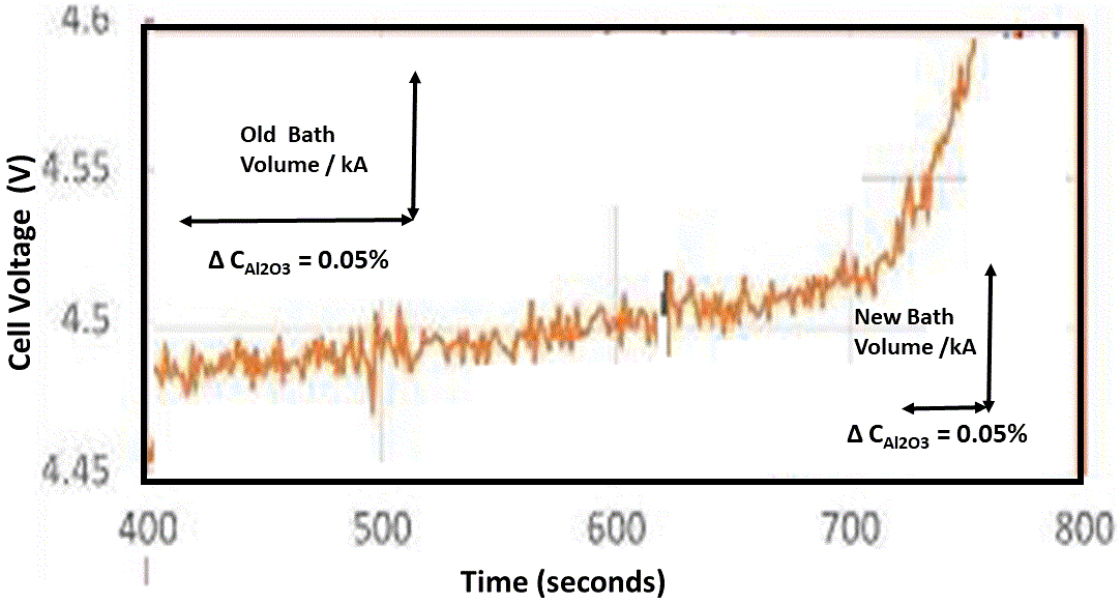

Figure 8. The rate of depletion of alumina in a low productivity high electrolyte volume cell compared with what it would be in a high productivity cell with reduced electrolyte volume / kA.

3. Increasing Potline Current and Cathode Performance

One of the main enablers for increasing productivity has been the lowering in cathode resistance by using materials of better electrical conductivity for both current collector bars and cathode blocks. This then allows an increase in cell current without a substantial impact on current efficiency, which would otherwise result from lowering the ACD spacing to maintain heat balance. One of the long-term established weaknesses of graphite has been a combination of porosity and the tendency to form intercalation compounds with, in this instance, sodium. Through the temperature and concentration gradients that exist within the cathode block these lead to secondary reactions that create products that exacerbate the overall wear. From multiple autopsies that have been performed on cells it is well established that preferential wear exists towards the ends of the more graphitized cathode blocks, with the wear increasing with cathodic current density.

As the wear holes are filled with liquid aluminium, this further exacerbates the unevenness in current distribution within the cathode block, as schematically illustrated in Figure 9. Despite the liquid aluminium levelling the current density at the upper surface of the metal pad, it results in an increase in horizontal current flows through the metal and therefore can generate waves and surface noise.

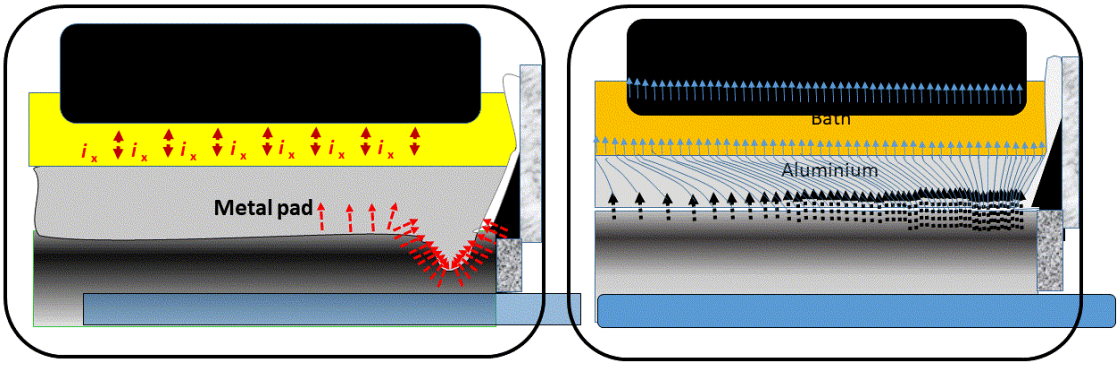

Figure 9. Illustrating the impact of the cathode wear (left) on the resulting model-predicted current distribution at the cathode-electrolyte interface for wear actually measured in a cell (right).

Using the wear measurements of the cathode block of the cell deliberately autopsied, in combination with the electrical properties of the current collector bar and cathode block materials, the change in the distribution of current along the cathode block surface has been calculated and is presented in Figure 10. Also of relevance the change in heat generation in the cathode block is presented .

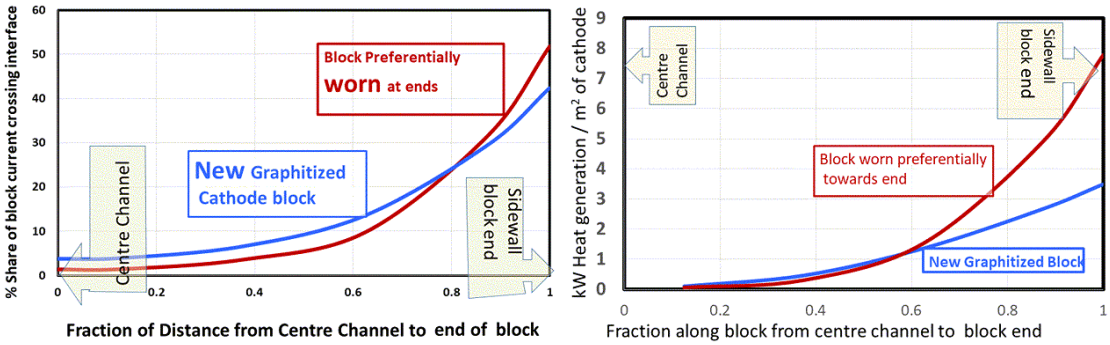

Figure 10. The change in current distribution between cathode block and metal pad with cathode wear (left), and the resulting variation in heat generation along the cathode block section (right).

It can be observed that the heat generation is substantial near the block-end of the cell which facilitates loss of side-ledge at the sidewall/metal pad zone whenever there is even a minor excursion in superheat. Once the ledge is removed, especially at the metal pad electrolyte interface, extra sodium co-deposition occurs because of the limited current that can flow through the rammed carbon and carbon insert. The following overall reaction is enabled at the electrolyte-carbon sidewall interface:

$$2Na_3AlF_6 + Al_2O_3 + 3C = 6Na + 4AlF_3 + 3CO(g) \qquad (4)$$

with this reaction having a ~0.1V lower cathode potential than aluminium deposition and the sodium being retained as intercalated NaC_x although it diffuses through to the colder sidewall. Ultimately the Na becomes visible, for example, by seeping through current collector bar windows forming NaOH and Na_2CO_3.

A further consequence of this reaction is a lowering in liquidus temperature through the higher aluminium fluoride concentration. This mitigates against ledge reforming unless there is a very

strong transverse electrolyte flow, which is less likely with the slotted anodes and low anode cathode distance.

4. Conclusions

The common consequence of the retrofits made to increase productivity, is an increase in the tendency to have spatial variability of cell conditions, by slowing down the flow and mixing of the electrolyte to the extent that concentration gradients are established, to the point where conditions approach or exceed those necessary for PFC co-evolution.

While productivity of the cells continues to increase, it comes with a general increase in the net energy consumption rate per unit production. Coupled with this are significant reductions in cell life compared with those achievable with more resistive cathode blocks, which tend to have a much more even cathodic current distribution and lower wear rate.

Redesign of cells coupled with changes in control and feeding strategy and the introduction of better sensors such as continuous individual anode current monitoring, should lead to better environmental and operating performance.

However the the design and wisdom of some of the changes introduced could benefit from re-assesment.

5. Acknowledgements

Special thanks to all the research students over the years, who have conducted systematic studies on operating cells and within the laboratory to help generate the data in support of this paper. Special mention of Drs. Daniel Whitfield, Jenny Purdie, Ali Zarouni, Ali Jassim, Rod Farr-Wharton, Sherilyn Hume, Mark Dorreen, Vanderlei Gusberti, Martin Iffert and Richard Haverkamp. Advice and assistance with the modelling aspects by Alexander Arkhipov and Dagoberto Severo are also greatly appreciated. And thanks to Halvor Kvande for critical editing and comments.

6. References

1. B. J. Welch, Technology of Electrolyte Reduction of Alumina by Hall-Heroult Process: I. A Voltage Analysis Under Conditions of Varying Alumina Concentrations. *Proc. Aust. I.M. & M.,* 214, (1965), 1-19.
2. O. Martin, R. Gariepy and G. Girault, APXe and AP60: The new reference for low energy and High Productivity Cells. *Proc. 11th Australasian Aluminium Smelting Conference*, Dubai, UAE, paper #40Th9, (2014).
3. J.M. Purdie, M. Bilek, M.P. Taylor, W.D. Zhang, B.J. Welch, B.J. and J.J.J. Chen, Impact of Anode Gas Evolution on Electrolyte Flow and Mixing in Aluminium Electrowinning Cells, *AIME Light Metals*, (1993), pp 355-360.
4. J.M. Purdie, Alumina behaviour and related process variation in all rolled cells for aluminium production, *PhD Thesis*, University of Auckland, (1993).
5. D. Whitfield, Aspects of Temperature in Aluminium Smelting, *PhD Thesis*, University of New South Wales, (2003).